Image Resolution and Signal-to-Noise Ratio Requirements for MR Imaging of Degenerative Cartilage

Joel D. Rubenstein[1]
Jonathan G. Li[2]
Sharmila Majumdar[3]
R. Mark Henkelman[1,2]

OBJECTIVE. The purpose of this study was to determine the MR image resolution and signal-to-noise ratio (SNR) required to reveal morphologic abnormalities in degenerative cartilage.

MATERIALS AND METHODS. In vitro MR microscopy of healthy bovine and degenerative human patellar cartilage was performed and image resolution degraded to simulate resolution achievable in routine and optimized clinical MR images. Noise was then added to images as in-plane resolution was increased to simulate the MR imaging appearance of cartilage with improved resolution, which is possible using a standard magnetic field strength. MR images of patellar cartilage from a healthy volunteer were also obtained to determine optimal SNR and image resolution achievable at 1.5 T; these images were compared with in vitro images to determine those features of abnormal cartilage that can be identified using available clinical MR imaging techniques.

RESULTS. In-plane resolution of 39 μm exquisitely defines degenerative changes in articular cartilage. As in-plane resolution decreases to 600 μm, only gross cartilage thinning and signal intensity alterations are seen. MR images simulating progressively improved resolution using higher field strength gradients with conventional field strengths and RF coils provided suboptimal information because of low SNR.

CONCLUSION. Routine clinical MR images do not accurately reveal early degenerative changes in articular cartilage; only large defects and distorted changes in the signal intensity of cartilage are seen.

American Journal of Roentgenology 1997;169:1089-1096.

Osteoarthritis is a degenerative disease of hyaline cartilage that ranks second only to cardiovascular disease as a cause of chronic disability [1]. Yet documenting the clinical diagnosis of osteoarthritis remains imprecise, especially in its early stages. As a result, efforts have been directed toward finding noninvasive methods to accurately detect degenerative changes in cartilage that could also be used to follow cartilage progression and response to therapy.

The early morphologic alterations of degenerative cartilage consist of superficial fraying and fibrillation of the normally smooth articular surface, accompanied by the formation of intrachondral clefts deep in relation to the articular surface [2]. With time, this structural deterioration may progress to more extensive vertical fissuring, surface abrasion, and tissue fragmentation, ultimately leading to significant cartilage loss.

Reports have described the role of MR imaging in defining abnormalities of hyaline cartilage [3–16]. Many of these studies have sought to identify the morphologic alterations that occur in degenerative cartilage, but with variable success. Most of these investigations have concentrated on finding optimal MR pulse sequences for the assessment of articular cartilage, primarily by selecting imaging parameters that accentuate the signal difference-to-noise ratio for cartilage, combined with techniques that maximize image resolution using available MR imaging technology.

Initial investigations focused on a variety of spin-echo and two-dimensional gradient-recalled echo sequences [3, 4]. Subsequent studies evaluated the role of magnetization transfer [5], MR arthrography [6], and three-dimensional (3D) gradient-recalled echo imaging [7, 8]. More recent reports have concluded that fat-suppressed 3D spoiled gradient-recalled acquisition in the steady state (spoiled GRASS) [9–14] and fast spin-echo [15, 16] sequences provide the best techniques for MR imaging of cartilage.

Received February 10, 1997; accepted after revision April 12, 1997.

[1]Department of Medical Imaging, University of Toronto, Sunnybrook Health Sciences Center, 2075 Bayview Ave., Toronto, Ontario M4N 3M5, Canada. Address correspondence to J. D. Rubenstein.

[2]Department of Medical Biophysics, University of Toronto, Sunnybrook Health Sciences Center, Toronto, Ontario M4N 3M5, Canada.

[3]Department of Radiology, University of California, 505 Parnassus Ave., San Francisco, CA 94143-0628.

AJR 1997;169:1089–1096

0361–803X/97/1694–1089

No investigation, to our knowledge, has established the image resolution and signal-to-noise ratio (SNR) that are required for accurate detection of the various morphologic changes in degenerative cartilage. This study was conducted to determine the requirements for these two MR imaging parameters and to assess whether they can be achieved.

Materials and Methods

High-Resolution In Vitro Imaging

Because of a lack of readily available samples of healthy human patellar cartilage, MR images of the patellar cartilage from a young (less than 2 years old) bovine knee were used to study the morphologic appearance of healthy articular cartilage. MR images of the patellar cartilage from five human cadaveric knees (73–91 years old at the time of death) were also used to study the morphologic changes of degenerative cartilage.

The bovine and human knee specimens were stored at –30°C. Before examination of each specimen, the intact knee was thawed in a refrigerated compartment (4°C) for 48 hr and then kept at room temperature (22°C) for 6 hr before study. The patella was dissected from the intact knee and a 1-cm cartilage–bone cube was cut with a band saw from either of the patellar facets. The sample was then placed in a plastic MR imaging tube and positioned with the planar surface of the cartilage perpendicular to the table. Images of the specimen were obtained with the planar surface of the cartilage facing the direction of the external magnetic field (B_0) and the coronal plane was chosen for imaging the sample, such that the frequency-encoding direction was left to right and the phase-encoding direction was superior to inferior.

MR imaging was performed with a 7.1-T system (Bruker CSI, Billerica, MA) using shielded-gradient coils (producing gradients to 85 gauss/cm) and a bandwidth of 100 kHz. T1-weighted images (TR/TE, 300/20) were obtained using a 256 × 256 matrix, 10-mm field of view, two signals averaged, and 1-mm section thickness (i.e., in-plane resolution of 39 × 39 μm).

Digital image data from selected 7.1-T MR images of the bovine and human specimens were then manipulated to simulate the appearance of cartilage at progressively lower resolutions (i.e., larger pixel dimensions) and to allow comparison of these images with clinical images of similar resolution. Poorer resolution images were simulated by taking the central 128 × 128, 64 × 64, 32 × 32, and 16 × 16 matrices of the respective original K-space data, followed by zero-filling of the high spatial frequencies of K-space before Fourier transformation to reconstruct the image. In all cases, magnitude images were reconstructed. This technique was used to simulate images with in-plane resolutions of 78 × 78 μm, 156 × 156 μm, 312 × 312 μm, and 624 × 624 μm, to ultimately approximate the resolution of routine clinical images of human patellar cartilage. All of the images were displayed with 256 × 256 pixels.

High-Resolution Clinical Imaging

MR images were obtained through the patellofemoral joint of a 34-year-old healthy male volunteer who claimed no history of injury or knee disease. To determine the optimal combination of SNR and image resolution, we obtained MR images with a 1.5-T system (Signa 5.5; General Electric Medical Systems, Milwaukee, WI) using three different coils (a commercial transmit–receive extremity coil, a phased array coil, and a 3-inch dual phased array coil) and two different image matrices (a 256 × 128 matrix with in-plane resolution of 390 × 780 μm, 0.75 signals averaged, and imaging

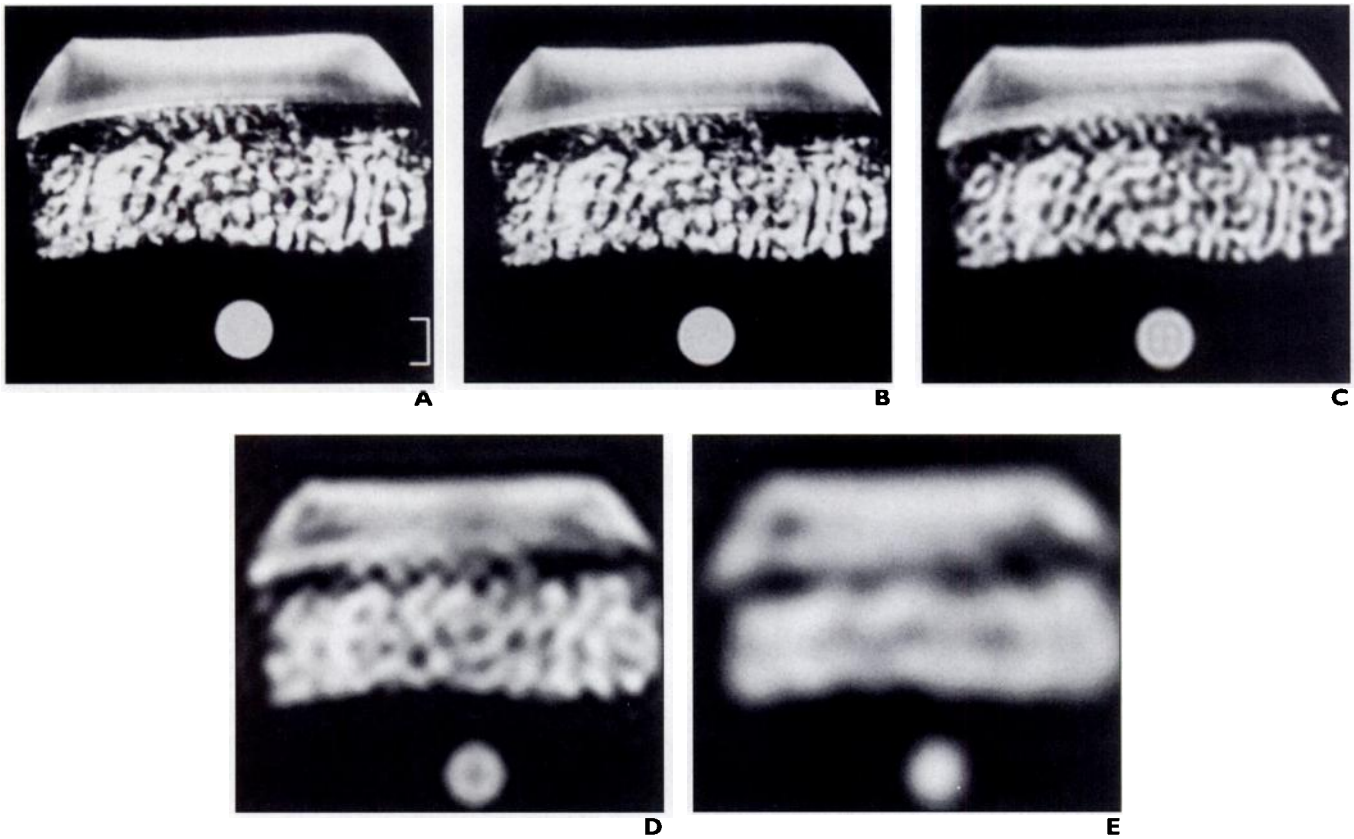

Fig. 1.—Healthy bovine cartilage–bone specimen obtained at 7.1 T. Cross-section of water-containing capillary tube is seen at bottom of each image. Lateral aspects of cartilage are curvilinear with distortion of signal intensity characteristics due to compression by margins of plastic MR tube.
A, T1-weighted spin-echo MR image with in-plane resolution of 39 × 39 μm; 1-mm scale is shown at right lower margin of image. Articular surface is smooth, and uncalcified cartilage is of uniform thickness with trilaminar appearance; architecture of subchondral trabecular bone is sharply defined.
B–E, T1-weighted spin-echo MR images show progressive loss of definition of articular surface, loss of trilaminar signal intensity of cartilage, and loss of subchondral bone. In-plane resolution in **B** = 78 × 78 μm, **C** = 156 × 156 μm, **D** = 312 × 312 μm, and **E** = 624 × 624 μm.

American Journal of Roentgenology 1997;169:1089-1096.

time of 2 min 37 sec; and a 512 × 256 matrix with in-plane resolution of 195 × 390 μm, two signals averaged, and imaging time of 13 min 43 sec). For each combination of coil and image matrix, MR images were obtained in the axial plane using a fat-suppressed T1-weighted 3D spoiled GRASS sequence (50/5, 30° flip angle, fractional echo, and 10-cm field of view through a 2.8-cm volume partitioned in 28 1-mm-thick sections), with the frequency-encoding direction left to right and the phase-encoding direction anterior to posterior.

Areas of 10 × 10 mm from the fat-suppressed 3D spoiled GRASS images of the healthy volunteer's lateral patellar facet were then selected that corresponded in size to those of the in vitro images. The images were displayed with 256 × 256 pixels using bilinear interpolation for optimal comparison with the in vitro images.

Effects of Image Resolution

The in vitro MR images of the healthy bovine cartilage and degenerative human cartilage with corresponding in-plane resolution were analyzed and compared in terms of surface fraying, fibrillation, fissuring, signal intensity characteristics, and cartilage thickness.

The clinical images were then examined and compared with the simulated in vitro images that had relatively similar image resolution (i.e., 195 μm with 156 μm and 390 μm with 312 μm) to identify those features of abnormal cartilage that can be interpreted.

Effects of SNR

The SNR was measured for each of the in vitro images and for the clinical images. Gaussian noise (i.e., spatially random) was then added to the in vitro images with in-plane resolution of 624 μm, such that the SNR was equivalent to the SNR achieved at 1.5 T with the best surface coil (i.e., the dual phased array coil). The SNR was then quartered for each doubling of image resolution (i.e., halving of pixel dimension) by adding random white noise to simulate image quality that could be achieved with increased gradient strength on a clinical examination. These clinically simulated images were then assessed to determine the impact of SNR in identifying the various features of osteoarthritic cartilage with each increment of improved image resolution.

Results

High-Resolution In Vitro Imaging

The highest resolution image (in-plane resolution of 39 × 39 μm) of the healthy bovine sample shows cartilage of uniform thickness with a smooth, well-defined articular surface and trilaminar signal intensity (i.e., a superficial lamina of bright signal intensity, an intermediate lamina of dark signal intensity, and a deep lamina of intermediate signal intensity); in addition, the subchondral bone shows well-defined trabeculae outlining the marrow space (Fig. 1A). As pixel size increases, the cartilage surface becomes increasingly blurred, with loss of definition of the trilaminar structure, and the osseous trabeculae–marrow space becomes more indistinct (Figs. 1B–1E).

MR images of three human cartilage samples show progressively advanced features of degenerative disease. The highest resolution image (in-plane resolution of 39 × 39 μm) of the first degenerative cartilage sample shows essentially uniform cartilage thickness, fraying of the articular surface with a deeper pit at one edge, and no distinct trilaminar structure (Fig. 2A). As pixel size increases, the fibrillated surface becomes indistinguishable from the MR imaging appearance of the healthy bovine sample with the largest pixel dimensions (624 × 624 μm) (Figs. 2B–2E). Ill-defined parallel hypointense lines in the cartilage, which decrease in number with increasing pixel dimensions, were also noted (Figs. 2C and 2D).

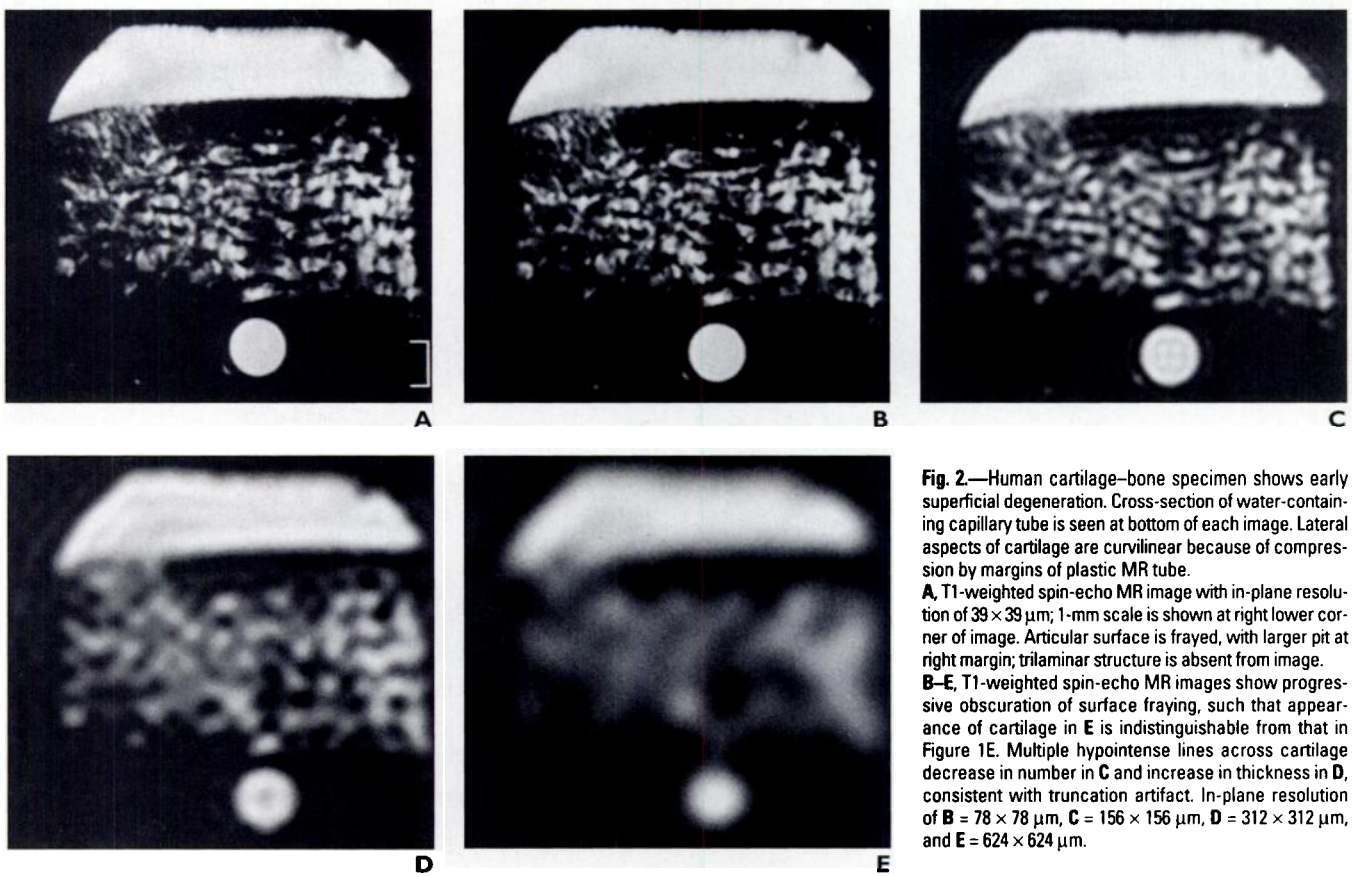

Fig. 2.—Human cartilage–bone specimen shows early superficial degeneration. Cross-section of water-containing capillary tube is seen at bottom of each image. Lateral aspects of cartilage are curvilinear because of compression by margins of plastic MR tube.
A, T1-weighted spin-echo MR image with in-plane resolution of 39 × 39 μm; 1-mm scale is shown at right lower corner of image. Articular surface is frayed, with larger pit at right margin; trilaminar structure is absent from image.
B–E, T1-weighted spin-echo MR images show progressive obscuration of surface fraying, such that appearance of cartilage in **E** is indistinguishable from that in Figure 1E. Multiple hypointense lines across cartilage decrease in number in **C** and increase in thickness in **D**, consistent with truncation artifact. In-plane resolution of **B** = 78 × 78 μm, **C** = 156 × 156 μm, **D** = 312 × 312 μm, and **E** = 624 × 624 μm.

The highest resolution image (in-plane resolution of 39 × 39 μm) of the second degenerative human cartilage sample shows a fibrillated articular surface with focal pits at one margin and sloped thinning of the cartilage from one side to the other (Fig. 3A). As the pixel size is increased, the frayed surface and focal fibrillation become imperceptible, and the cartilage thinning becomes less apparent (Figs. 3B–3E). Similar to the first sample of degenerative cartilage, ill-defined parallel hypointense lines in the cartilage are noted that decrease in number with increasing pixel dimensions (Fig. 3C).

The highest resolution image (in-plane resolution of 39 × 39 μm) of the third degenerative human cartilage sample shows an irregular frayed articular surface, loss of uniform cartilage thickness, an intrasubstance cleft dissecting below the articular surface of the cartilage, and heterogeneous signal intensity without obvious laminar structure (Fig. 4A). As pixel dimensions increase, the cartilage surface becomes blurred, such that the fraying is no longer seen, only gross undulation of the surface is apparent, and the intrachondral cleft becomes less distinct and ultimately appears as an area of decreased signal intensity in the cartilage (Figs. 4B–4E).

High-Resolution Clinical Imaging

The 3D volume images show that the patellar cartilage is of uniform thickness with enhanced contrast, compared with the fat-suppressed signal intensity of bone, irrespective of the coil or image matrix (Figs. 5A–5D). For the images with a 256 × 128 matrix, the SNR showed a progressive increase when the extremity coil (SNR = 13) (Fig. 5A) was compared with the phased array coil (SNR = 18) (Fig. 5B) and the dual phased array coil (SNR = 32) (Fig. 5C). A similar increase in SNR for these coils was seen in the 512 × 256 matrix images (SNR of 4 for the extremity coil, versus 6.6 for the phased array coil, and 15 for the dual phased array coil) (Fig. 5D), but the effective SNR achieved with each coil is less because of the increased noise resulting from the smaller pixels.

Examination of the insets focused on the lateral patellar facet that shows a fuzzy articular surface with repeated shallow undulations. The trilaminar signal intensity of the cartilage is apparent in each of the 256 × 128 images (Figs. 5E–5G) but is best defined with the phased array coils; this trilaminar appearance is barely perceptible in the smaller pixel images (512 × 256 matrix) (Fig. 5H). The extremity-coil image is objectionably noisy compared with images using the phased array systems that show better SNR.

Effects of Image Resolution

Evaluation of the cartilage surface requires a minimum in-plane image resolution of 156 μm to distinguish fraying and fibrillation of the articular surface from a normal smooth surface, although larger pits are visible with 312 μm resolution (Figs. 1–4).

The intrachondral fissure remains visible with an in-plane resolution of 156 μm (Fig. 4C), but with larger in-plane dimensions the cleft becomes distorted in appearance, resulting in a focus of decreased signal intensity simulating a full-thickness defect in the cartilage (Figs. 4D and 4E).

Gross thinning of the cartilage is apparent even with the largest in-plane pixel dimen-

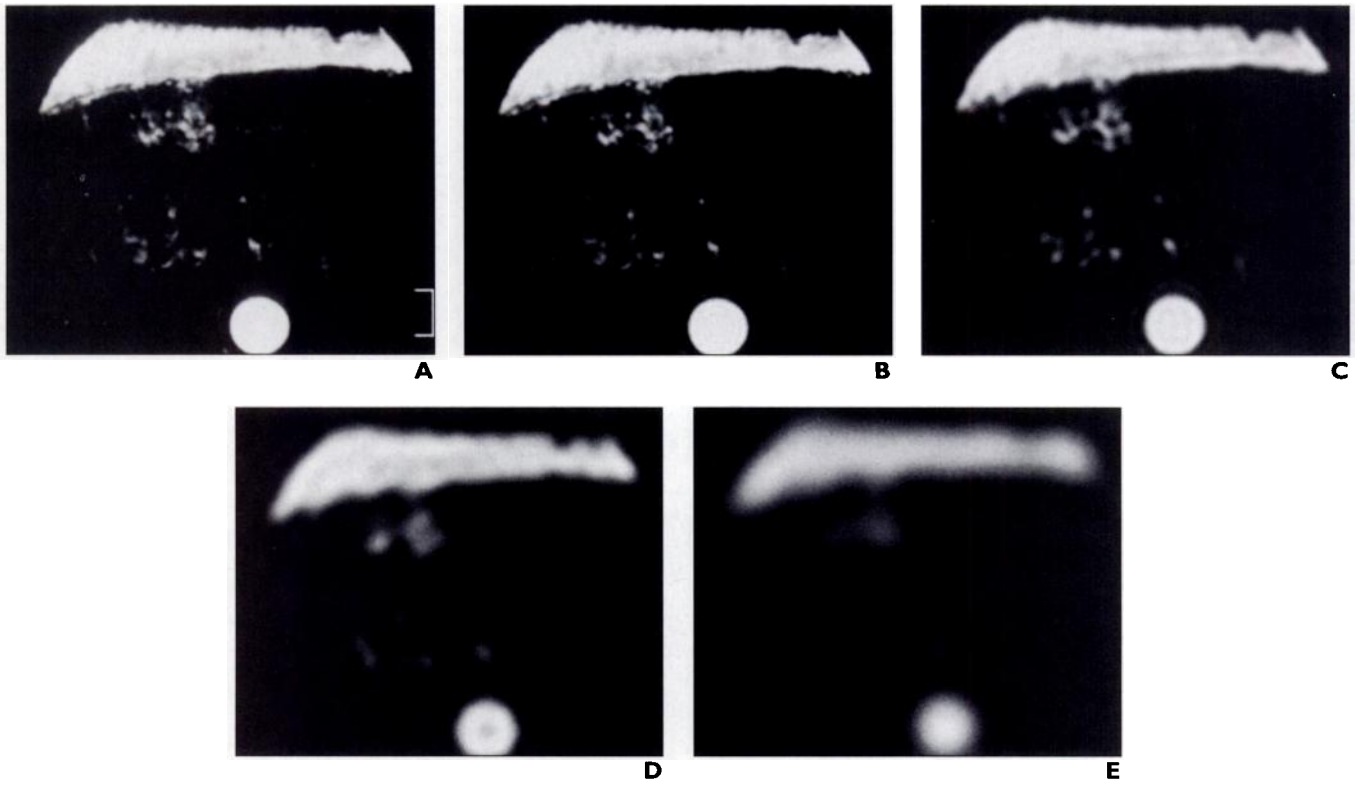

Fig. 3.—Human cartilage–bone specimen shows moderate superficial degeneration. Cross-section of water-containing capillary tube is seen at bottom of each image. Lateral aspects of cartilage are curvilinear because of compression by margins of plastic MR tube.
A, T1-weighted spin-echo MR image with in-plane resolution of 39 × 39 μm; 1-mm scale is shown at right lower corner of image. Articular surface is frayed, with fibrillation on right and gradual thinning of cartilage from left to right.
B–E, T1-weighted spin-echo MR images show surface irregularities that are progressively obscured, although cartilage thinning from left to right is still apparent. Truncation artifact is again present and is best seen in **C**. In-plane resolution of **B** = 78 × 78 μm, **C** = 156 × 156 μm, **D** = 312 × 312 μm, and **E** = 624 × 624 μm.

sions. Visualization of the trilaminar signal intensity of healthy bovine articular cartilage remains possible with an in-plane resolution of 312 μm but disappears with an in-plane resolution of 624 μm.

Comparison of the clinical images (in-plane resolutions of 390 μm and 195 μm) (Figs. 5G and 5H) with the in vitro images of comparable resolution (in-plane resolutions of 156 μm and 312 μm) (Figs. 1C and 1D) shows an appearance of the articular cartilage that is similar in terms of surface detail and signal intensity characteristics.

Effects of SNR

To represent the SNR in an optimized clinical image, Gaussian noise was added to the image in Figure 4E until an SNR of 76 was achieved, which would approximate the expected SNR obtained using the imaging parameters in Figure 5D at a resolution of 624 × 624 μm (Fig. 6A). When resolution was amplified to in-plane dimensions of 312 μm and SNR was reduced fourfold to an SNR of 19 (Fig. 6B), the resultant image was similar in appearance to Figure 4D; however, with further doubling of resolution (i.e., halving of pixel size) and quartering of SNR, the resulting image became objectionably noisy with marked loss of diagnostic information (Fig. 6C). With the last incremental improvement in resolution and increase in noise, only the outline of the specimen was visible through the noise (Fig. 6D). This finding is consistent with a study that showed that SNR should be spent to achieve improved resolution for better visibility until the SNR is decreased to approximately 20 [17]; beyond this level, further decrease in SNR to obtain better resolution simply results in the image breaking into "salt and pepper" noise.

Discussion

Normal hyaline cartilage is a hydrated gel with a smooth articular surface covered by a synovial fluid lubricant to permit almost frictionless movement of diarthrodial joints [18]. Degenerative changes of articular cartilage interfere with the normal function of these joints, and the pathologic alterations that occur have been divided into superficial and basal degeneration [2].

Superficial degeneration is age dependent and shows increasing prevalence with advancing age. The earliest features consist of fraying and flaking of the tangential zone at the articular surface of the cartilage. Extension of these discontinuities into the deeper radial zone of cartilage is referred to as fibrillation, and scanning electron microscopy has shown that the fronds created by cartilage fibrillation range in height from 20 to 150 μm [19]. As a result of continued load-bearing and shearing forces, these fibrillated areas of cartilage become subject to abrasion and fragmentation that may ultimately denude areas of subchondral bone. Although evidence of superficial degeneration is commonly found at the articular margins of cartilage in young asymptomatic patients, extension of this process to areas of repetitive patellofemoral contact is believed to correlate

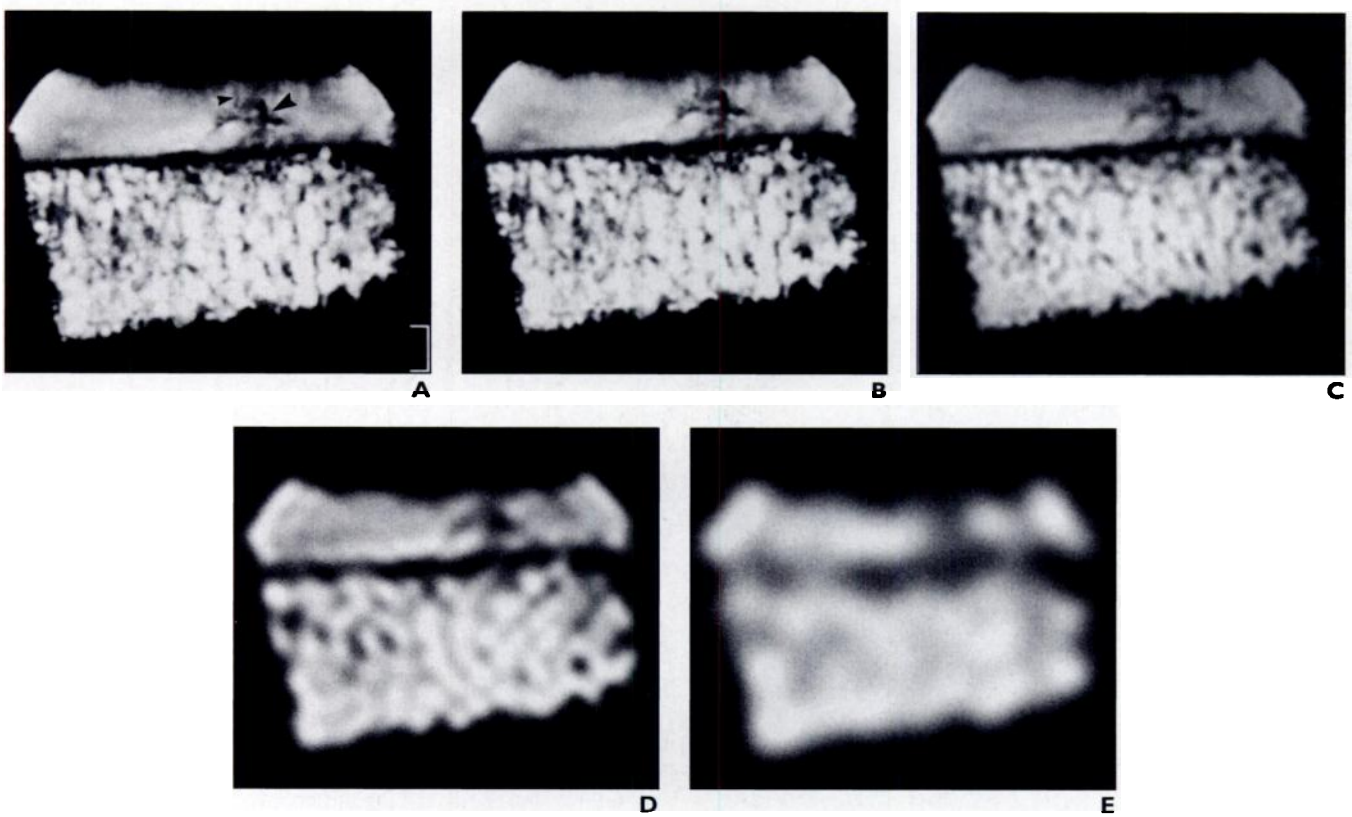

Fig. 4.—Human cartilage–bone specimen shows superficial and basal degeneration. Lateral aspects of cartilage are curvilinear because of compression by margins of plastic MR tube.

A, T1-weighted spin-echo MR image with in-plane resolution of 39 × 39 μm; 1-mm scale is shown at right lower corner of image. Cartilage surface is fibrillated, and cruciate-shaped intrachondral fissure (*large arrowhead*) is present at right of midline, with fine fissure communicating with articular surface (*small arrowhead*).

B–E, T1-weighted spin-echo MR images show fibrillated surface becoming progressively blurred and intrachondral fissure becoming distorted and indistinct, such that fissure simulates full-thickness vertical cleft extending to articular surface in **E**. Truncation artifact is seen in **C** and **D**. In-plane resolution of **B** = 78 × 78 μm, **C** = 156 × 156 μm, **D** = 312 × 312 μm, and **E** = 624 × 624 μm.

American Journal of Roentgenology 1997.169:1089-1096.

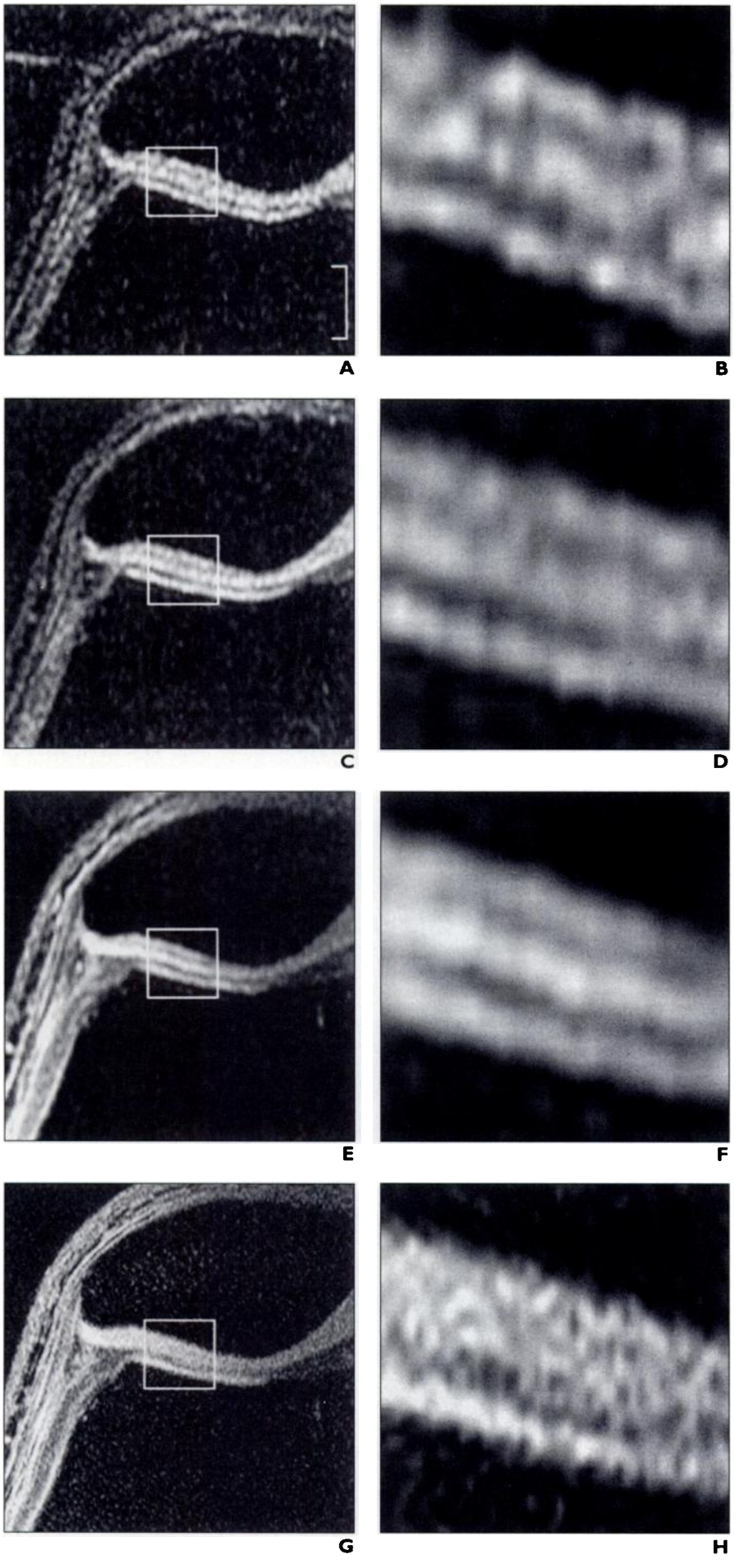

Fig. 5.—Patellar cartilage from healthy volunteer using different combinations of imaging coils and resolution. Insets represent 10 × 10 mm area in lateral patellar facet, corresponding in size to in vitro images. Fuzzy articular surface of each image is seen; morphologic appearance of cartilage is similar to in vitro images with in-plane resolution between 312 and 624 μm. Images obtained with extremity coil show objectionably low signal-to-noise ratio (SNR), and phased array coil image shows optimal SNR.

A, Three-dimensional spoiled gradient-recalled acquisition in the steady state (spoiled GRASS) axial MR image (60/5 [TR/TE], 30° flip angle, 10-cm field of view, two excitations, 256 × 128 matrix) using extremity coil (in-plane resolution, 390 × 780 μm; SNR = 13). One-centimeter scale is shown at right lower margin of image.

B, MR image corresponds to 10 × 10 mm inset of lateral patellar facet, corresponding in size to in vitro image **A**.

C, Three-dimensional spoiled GRASS axial MR image (60/5, 30° flip angle, 10-cm field of view, two excitations, 256 × 128 matrix) using phased array coil (in-plane resolution, 390 × 780 μm; SNR = 18).

D, MR image corresponds to 10 × 10 mm inset from **C**.

E, Three-dimensional spoiled GRASS axial MR image (60/5, 30° flip angle, 10-cm field of view, two excitations, 256 × 128 matrix) using dual phased array coil (in-plane resolution, 390 × 780 μm; SNR = 32).

F, MR image corresponds to 10 × 10 mm inset from **E**.

G, Three-dimensional spoiled GRASS axial MR image (60/5, 30° flip angle, 10-cm field of view, two excitations, 512 × 256 matrix) using dual phased array coil (in-plane resolution, 195 × 390 μm; SNR = 15).

H, MR image corresponds to 10 × 10 mm inset from **G**. This image (512 × 256 matrix) has higher resolution but shows unacceptably low SNR compared with **F** (256 × 128 matrix).

American Journal of Roentgenology 1997.169:1089-1096.

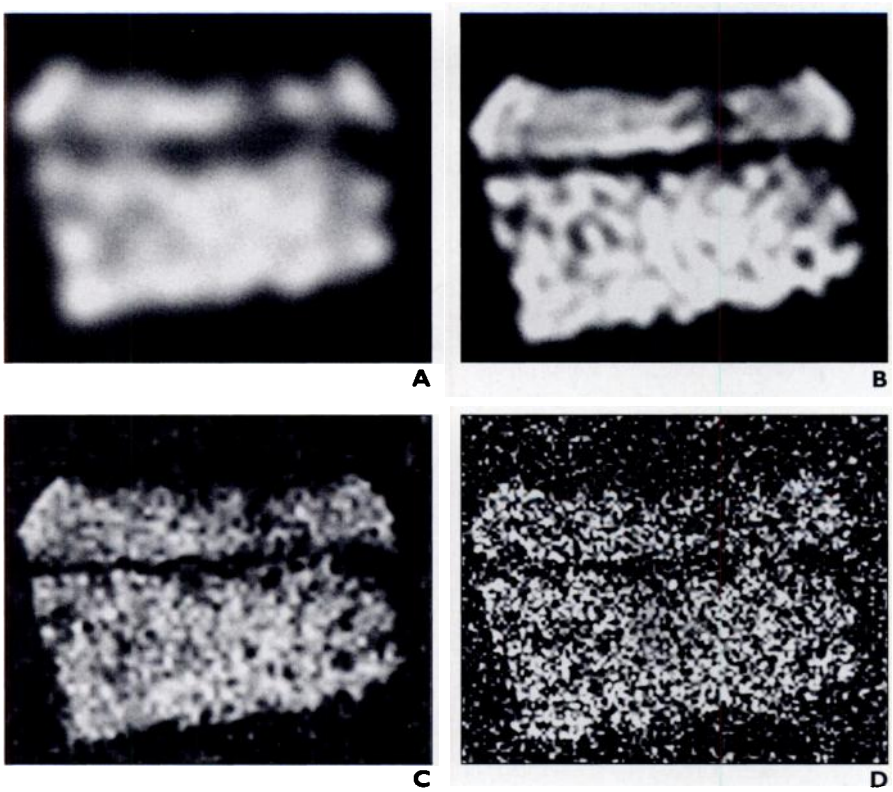

Fig. 6.—MR images show effect of signal-to-noise ratio (SNR) with decreasing pixel sizes at 1.5 T.
A, Image corresponds to Figure 4E (in-plane resolution, 624 × 624 μm), but noise has been added to decrease SNR to 76 to approximate SNR of clinical image obtained with dual phased array coil.
B, Image corresponds to Figure 4D (in-plane resolution, 312 × 312 μm), but noise has been added to decrease SNR by four times that of **A**.
C, Image corresponds to Figure 4C (in-plane resolution, 156 × 156 μm), but noise has been added to decrease SNR by four times that of **B**. Image has objectionably low SNR, with unacceptable loss of information.
D, Image corresponds to Figure 4B (in-plane resolution, 79 × 79 μm), but noise has been added to decrease SNR by four times that of **C**. Only outline of specimen is visible through excessive noise.

with the development of pain associated with histologic features of osteoarthritis.

Basal degeneration develops in the deep layers of hyaline cartilage, beginning with fasciculation of the radially oriented collagen, and is manifest only as an area of focal softening attributed to localized edema. Histologic examination of cartilage at this stage reveals fissures in the deep portion of the cartilage beneath the area of softening. With time, fissures in the deep layer of cartilage may lead to the rupture of the overlying tangential collagen fibers or, less commonly, result in a superficial blister at the articular surface.

Using MR imaging, researchers have attempted to identify the various features of degenerative change in cartilage and, in some cases, have tried to correlate the MR findings with arthroscopy or pathologic staging systems [3–16]. These studies have specifically endeavored to examine signal intensity changes in the cartilage as well as morphologic alterations that include surface fraying, fibrillation, fragmentation, and ulceration; fissures that may be intrachondral, may extend to the articular surface, or that underlie a blister at the articular surface; and varying degrees of cartilage thinning that may ultimately lead to exposure of the subchondral bone.

Recent reports have examined the use of fat-suppressed imaging in conjunction with thin-partition 3D spoiled GRASS imaging to provide maximal spatial resolution and high contrast [9–14]. We agree that this approach is of value in maximizing MR image contrast, but the results of our study suggest that the image resolution achieved with this and similar techniques may not be adequate for the depiction of degenerative cartilage, especially in the presence of early morphologic changes. Compared with conventional two-dimensional spin-echo imaging, the use of 3D imaging produces smaller voxels by decreasing the slice thickness, but in-plane resolution is similar to that of most spin-echo images (i.e., 625 μm or larger pixel dimensions). Using fat-suppressed 3D techniques, researchers have recently achieved in-plane resolution as high as 469 μm (i.e., in only one direction), although other researchers have used 546–625 μm as the maximal one-direction in-plane resolution [9–14]. Fast spin-echo techniques have also achieved image resolution ranging from 390 to 500 μm in one plane [15, 16].

Our data show that image resolution of this order is inadequate to reveal fraying of the articular surface of cartilage, and that the smooth articular surface of healthy cartilage is indistinguishable from early superficial changes of degenerative cartilage. More advanced fibrillation and focal pitting of the articular surface require maximum pixel dimensions of 150 μm. In-plane resolution of approximately 300 μm is capable of showing large pits in the articular surface and areas of major cartilage thinning, but our findings suggest that a pixel size larger than 300 μm does not reliably show superficial alterations of articular cartilage.

With regard to basal degeneration of cartilage, our results indicate that reliable depiction of intrachondral fissures requires a maximum pixel size of 150 μm. Pixel sizes that exceed this level may show focal alteration in cartilage signal intensity, even with an in-plane resolution of 625 μm, but the image shows an increasingly distorted appearance of the true morphologic abnormality.

The impact of SNR is important in considering methods for improving the spatial resolution in clinical MR images of cartilage. If the field strength of clinical imagers continues to be in the range of 1.5 to 2.0 T, our results would suggest that attempts to enhance image resolution through gradient improvements alone may not provide satisfactory cartilage depiction because of the decrease in SNR that would result. The SNR problem can be partially solved with the use of specialized coils, as we have shown, and with various pulse sequences (e.g., fast spin echo) to enhance SNR for given imaging times; however, we believe more investigation is needed to determine if

these solutions are sufficient for routine clinical imaging.

An additional limitation of improved spatial resolution in MR images is the loss of low contrast detectability for a constant imaging time [20]. This effect is illustrated in our study by comparing the dual phased array clinical image with the 256 × 128 matrix (SNR = 32) (Figs. 5C and 5G) with the 512 × 256 matrix image (SNR = 15) (Figs. 5D and 5H). The trilaminar appearance of cartilage in fat-suppressed 3D spoiled GRASS images has been attributed to truncation artifact when the cartilage is spanned by approximately four pixels [21]. The presence of this artifact is supported in our study by the apparent absence of the laminar structure on the higher resolution image (512 × 256 matrix); however, careful review of this higher resolution image also shows an objectionably low SNR that interferes with the reliable interpretation of signal intensity alterations within the cartilage.

In summary, our investigation shows that careful attention must be paid to optimizing image resolution and SNR when obtaining MR images of articular cartilage. We believe that previous studies have been unable to accurately define early morphologic abnormalities of cartilage because contemporary MR imaging technology does not offer practical techniques to obtain the ideal image resolution with acceptable SNR. This goal may be attainable with the development of higher sensitivity receiver coils used in conjunction with clinical magnets operating at field strengths above 4 T.

Acknowledgments

We thank G. Allan Johnson of Duke University Medical Center for expert assistance in obtaining the MR microscopy images. We also gratefully acknowledge support from the National Cancer Institute of Canada and General Electric Medical Systems of Canada.

References

1. Peyron JG. Osteoarthritis: the epidemiologic viewpoint. *Clin Orthop* **1986**;213:13–19
2. Goodfellow J, Hungerford DS, Woods C. Patello-femoral joint mechanics and pathology. 2. Chondromalacia patellae. *J Bone Joint Surg Br* **1976**; 58-B:291–299
3. Konig H, Sauter R, Deimling M, Vogt M. Cartilage disorders: comparison of spin-echo, CHESS and FLASH sequence MR images. *Radiology* **1987**; 164:753–758
4. Hayes CW, Sawyer RW, Conway WF. Patellar cartilage lesions: in vitro detection and staging with MR imaging and pathologic correlation. *Radiology* **1990**;176:479–483
5. Wolff SD, Chesnick S, Frank JA, Lim KO, Balaban RS. Magnetization transfer contrast: MR imaging of the knee. *Radiology* **1991**;179:623–628
6. Kramer J, Recht MP, Imhof H, Engel A. MR contrast arthrography (MRA) in assessment of cartilage lesions. *J Comput Assist Tomogr* **1994**;18: 218–224
7. Heron CW, Calvert PT. Three-dimensional gradient-echo MR imaging of the knee: comparison with arthroscopy in 100 patients. *Radiology* **1992**; 183:839–844
8. Hardy PA, Recht MP, Piraino D, Thomasson D. Optimization of a dual echo in the steady state (DESS) free-precession sequence for imaging cartilage. *J Magn Reson Imaging* **1996**;6:329–335
9. Recht MP, Kramer J, Marcelis S, et al. Abnormalities of articular cartilage in the knee: analysis of available MR techniques. *Radiology* **1993**;187: 473–478
10. Peterfy CG, Majumdar S, Lang P, van Dijke CF, Sack K, Genant H. MR imaging of the arthritic knee: improved discrimination of cartilage, synovium and effusion with pulsed saturation transfer and fat-suppressed T1-weighted sequences. *Radiology* **1994**;191:413–419
11. Disler DG, Peters TL, Muscoreil SJ, et al. Fat-suppressed spoiled GRASS imaging of knee hyaline cartilage: technique optimization and comparison with conventional MR imaging. *AJR* **1994**;163: 887–892
12. Disler DG, McCauley TR, Wirth CR, Fuchs MD. Detection of knee hyaline cartilage defects using fat-suppressed three-dimensional spoiled gradient-echo MR imaging: comparison with standard MR imaging and correlation with arthroscopy. *AJR* **1995**;165:377–382
13. Recht MP, Piraino DW, Paletta GA, Schils JP, Belhobek GH. Accuracy of fat-suppressed three-dimensional spoiled gradient-echo FLASH MR imaging in the detection of patellofemoral articular cartilage abnormalities. *Radiology* **1996**;198: 209–212
14. Disler DG, McCauley TR, Kelman CG, et al. Fat-suppressed three-dimensional spoiled gradient-echo imaging of hyaline cartilage defects in the knee: comparison with standard MR imaging and arthroscopy. *AJR* **1996**;167:127–132
15. Broderick LS, Turner DA, Renfrew DL, Schnitzer TJ, Huff JP, Harris C. Severity of articular cartilage abnormality in patients with osteoarthritis: evaluation with fast spin-echo MR vs arthroscopy. *AJR* **1994**;162:99–103
16. Rose PM, Demlow TA, Szumowski J, Quinn SF. Chondromalacia patellae: fat-suppressed MR imaging. *Radiology* **1994**;193:437–440
17. Owen RS, Wehrli FW. Predictability of SNR and reader preference in clinical MR imaging. *Magn Reson Imaging* **1990**;8:737–745
18. Haberman D. The biology of osteoarthritis. *N Engl J Med* **1989**;320:1322–1330
19. Minns RJ, Steven FS, Hardinge K. Osteoarthritic articular cartilage lesions of the femoral head observed with scanning electron microscopy. *J Pathol* **1977**;122:63–70
20. Constable RT, Henkelman RM. Contrast, resolution, and detectability in MR imaging. *J Comput Assist Tomogr* **1991**;15:297–303
21. Erickson SJ, Waldschmidt JG, Czervionke LF, Prost RW. Hyaline cartilage: truncation artifact as a cause of trilaminar appearance with fat-suppressed three-dimensional spoiled gradient-recalled sequences. *Radiology* **1996**;201:260–264